A static compressible flow model of synthetic jet actuators

H. Tang and S. Zhong
School of Mechanical, Aerospace and Civil Engineering,
The University of Manchester
Manchester, UK

ABSTRACT

In this paper, a simple static compressible flow model for circular synthetic jet actuators is described. It is used to undertake a systematic computational investigation of the effect of changing actuator geometrical and operating parameters on the magnitude of peak jet velocity at the orifice exit of an actuator whose diaphragm displacement and frequency are allowed to vary independently. It is found that, depending on the flow conditions inside the orifice duct, the actuator may operate in two distinct regimes, i.e. the Helmholtz resonance regime and the viscous flow regime. In the Helmholtz resonance regime, the resultant synthetic jet is generated by the mass physically displaced by the oscillating diaphragm coupled with the Helmholtz resonance in the actuator. In the viscous flow regime, the Helmholtz resonance is completely damped by viscous effect such that the jet is produced by the diaphragm oscillation alone. The relationship between actuator geometrical and operating parameters at the optimum condition which yields the maximum peak jet velocity at a given diaphragm displacement is also established for these two regimes. Finally, a preliminary procedure for designing synthetic jet actuators for flow separation control on an aircraft wing is proposed.

NOMENCLATURE

a	speed of sound, ms^{-1}
D	diameter of diaphragm, cavity, or orifice, mm
f	oscillation frequency of diaphragm, Hz
h	depth of orifice, mm
H	height of cavity, mm
p	pressure, N/m^2
r	radius of diaphragm and cavity, mm
R	universal gas constant, kJ/kg K
u	instantaneous velocity, ms^{-1}
γ	ratio of specific heats
Δ	peak-to-peak displacement at the diaphragm centre, mm
μ	dynamic viscosity, kg/m s
ν	kinematic viscosity, m^2/s
ρ	density, kg/m^3
Π	pressure gradient, N/m^3

Subscripts

c	cavity value
H	value for the Helmholtz resonance regime
inv	inviscid flow value

Paper No. 3081. Manuscript received 27 March 2006, revised 3 March 2007, accepted 4 May 2007.

https://doi.org/10.1017/S0001924000004681 Published online by Cambridge University Press

max	maximum value
o	orifice value
opt	optimum value
peak	peak jet value
v	value for the viscous flow regime

1.0 INTRODUCTION

There has been an intense research on synthetic jets in the last ten years due to their potential use in flow control on aircraft[1-4]. An application of great interest is to delay flow separation on the flap of a multi-element high-lift system at take-off and landing by employing an array of synthetic jets. Synthetic jets have the advantage over conventional vortex generators in that their strength can be adjusted based on demand and there is no protrusion to the flap surface that requires an extra flap gap to accommodate[5].

A substantial progress in understanding the characteristics of macro-scale synthetic jets in quiescent conditions and their impact on separating boundary layers has been made[2,4]. For MEMS-based synthetic jet actuators to be used at flight conditions, their orifice diameter is likely to be in the range of a few hundredths to a few tenths of a millimeter[6]. In these micro-scale actuators the compressibility and viscosity effect are expected to be significant and the characteristics of these synthetic jets may not be similar to those of their macro-scale counterparts. At present, since measurements of micro-scale jets with adequate resolution still present a technical challenge, experimental data that can be used to assist the geometrical optimisation of these actuators for maximum flow control effectiveness are scarce. Hence theoretical studies of the effect of actuator geometry on the performance of micro-scale jets should be undertaken to bridge this gap, with the ultimate goal of developing a design methodology for synthetic jet actuators for flow separation control at full-scale flight conditions.

As shown in Fig. 1, a typical circular synthetic jet actuator consists of three key components: an oscillating diaphragm, a circular orifice with a finite depth, and a cylindrical cavity. The oscillation of the diaphragm generates a small pressure difference between the cavity and the ambient. This pressure difference is manifested as a pressure gradient along the orifice duct that drives the fluid inside the cavity out of the orifice in the form of a jet. The peak jet velocity, achievable at the orifice exit during the diaphragm oscillation cycle, is a key measure of the impact of the synthetic jet on an external flow. The jet velocity is expected to be affected strongly by the fluid dynamics inside the actuator and its geometry. An optimal design of the actuator should yield a maximum peak jet velocity for a given actuator operating condition.

The fluid flow in the cavity and orifice duct can be simulated using existing commercial CFD codes which solve the full Navier-Stokes equations. However, the amount of computation makes the task of identifying the optimal actuator design for a specific application impractical due to the large number of design variables involved. By introducing adequate assumptions, the flow in the actuator can be modeled using simplified governing equations. A parametric study of the actuator can then be carried out systematically, providing an insight of the effects of actuator geometry on the performance of the synthetic jets. This is the driver behind the development of low-dimensional actuator performance prediction models, including the model presented in this paper.

Some low-dimension computational models have already been reported in the literature. Tang and Zhong[7] have developed a prediction model for synthetic jet actuators assuming that the flow inside the cavity is incompressible and the flow in the orifice duct is inviscid. The model gives reliable prediction of the characteristics of synthetic jets for an actuator with an orifice diameter of 5mm. However it over-predicts the jet velocity when the orifice diameter is reduced to less than 1mm due to the onset of compressibility and viscosity effect in the actuator. Rathnasingham and Breuer[8] developed a simplified computational model which consists of a system of coupled equations describing the fluid-structural behavior. The compressibility effect and viscosity of the flow in the actuator were included in the model. They characterised the viscous effects by the Stokes number and found an optimal operating Stokes number by matching the viscous flow solution to an ideal, inviscid flow solution. Their idea was later adopted by Lockerby and Carpenter[9] who developed a new computational model which was capable of predicting an optimal cavity height and orifice diameter that was close to experimental observations[2].

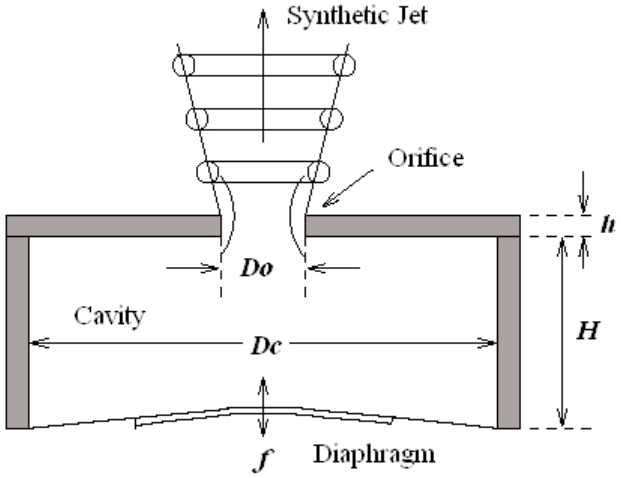


Figure 1. Schematic of synthetic jet actuator.

In this paper, the computational model developed by Lockerby and Carpenter[9] is modified and employed to study the effects of various actuator geometrical parameters and operating conditions on the magnitude of peak jet velocity at the orifice exit. An attempt is made to establish the relation among these parameters at the optimum condition which yields the maximum peak jet velocity at a given diaphragm displacement. A procedure for designing synthetic jet actuators for flow separation control on an aircraft wing is also proposed.

2.0 THE ACTUATOR MODEL

For a typical circular synthetic jet actuator as shown in Fig. 1, its performance is determined by four actuator geometrical parameters: orifice diameter (D_o), orifice depth (h), cavity diameter (D_c) and cavity depth (H); two actuator operating parameters: oscillation amplitude (Δ) and oscillation frequency (f); and three fluid parameters: temperature (T), density (ρ) and viscosity (v). In the present work, the changes in temperature and viscosity are not considered and the models focus on predicting how the peak jet velocity varies upon changes in actuator geometrical parameters and actuator operating parameters.

In this paper, two mathematical models will be discussed, i.e. the static compressible model (SC Model) originally developed by Lockerby and Carpenter[9] and the dynamic incompressible model (DI Model) derived by Tang and Zhong[7]. The DI model is a much simpler model which provides a calibration of the SC model in the incompressible flow regime.

2.1 The static compressible model (SC model)

In the SC model, the flows in the cavity and orifice duct are considered to be compressible and are modelled separately. In the original model developed by Lockerby and Carpenter[9], the

https://doi.org/10.1017/S0001924000004681 Published online by Cambridge University Press

diaphragm is assumed to vibrate at its natural frequency. However, in the modified model presented in this paper, the diaphragm frequency and displacement are allowed to vary independently so that an optimal frequency can also be identified.

2.1.1 The diaphragm

In the present study, the diaphragm is clamped round its circular edge and its oscillating frequency and displacement at the centre can be set independently. According to the theory of plates and shells[10], the instantaneous shape of the diaphragm which undergoes a sinusoidal motion is described as

$$\delta(r,t)=\frac{\Delta}{2}\left[1-\frac{r^2}{r_c^2}+\frac{2r^2}{r_c^2}\ln\left(\frac{r}{r_c}\right)\right]\mathrm{Sin}(2\pi ft) \quad \ldots (1)$$

where δ is the diaphragm deformation relative to its neutral position, r is the radial distance from the diaphragm centre, r_c is the radius of the diaphragm, and Δ is the peak-to-peak displacement at the centre. This model neglects the impact of the pressure difference exerted across the diaphragm which may restrain its movement.

2.1.2 The orifice

For simplicity, the flow in the orifice duct is assumed to be parallel. The Navier-Stokes equations for axisymmetric parallel flows are given by

$$\begin{cases} \dfrac{\partial\rho}{\partial t}+\dfrac{\partial(\rho u)}{\partial x}=0 & \ldots (2) \\ \dfrac{\partial(\rho u)}{\partial t}+\dfrac{\partial(\rho u^2)}{\partial x}=-\dfrac{\partial p}{\partial x}+\mu\nabla^2 u & \ldots (3) \end{cases}$$

where x is the axial coordinate, t is time, u is the axial velocity, and ∇^2 is the Laplacian operator given by

$$\nabla^2\equiv\left[\frac{1}{r}\frac{\partial}{\partial r}+\frac{\partial^2}{\partial r^2}\right] \quad \ldots (4)$$

For low-speed flows, the changes in the pressure p, density ρ and velocity u along the orifice duct are small hence a linear spatial variation can be adequately assumed. As such Equations (2) and (3) are simplified as

$$\begin{cases} u_2=\dfrac{\rho_1 u_1}{\rho_2}-\dfrac{h}{2\rho_2}\dfrac{\partial\rho_1}{\partial t} & \ldots (5) \\ \dfrac{\partial u_1}{\partial t}+\left(\dfrac{\rho_1}{\rho_2}-1\right)\dfrac{u_1^2}{h}-\dfrac{u_1}{2\rho_2}\dfrac{\partial\rho_1}{\partial t}=\dfrac{p_1-p_2}{\rho_1 h}+\dfrac{\mu}{\rho_1}\nabla^2 u_1 & \ldots (6) \end{cases}$$

where the subscripts 1 and 2 denote values at the inlet and outlet, respectively. In Equation (6), u_1 is the only unknown variable once p_1 and ρ_1 are obtained from the subsequent cavity model. Note that the fluid at the outlet (corresponding to the subscript 2) is assumed to be incompressible and the density variation occurs only within the cavity and orifice.

2.1.3 The cavity

The cavity is the lever between the diaphragm motion and jet expulsion. Its behaviour is central to the actuator system. Based on mass conservation in the cavity, the variation of the mass in the cavity can be expressed as

$$\frac{dM_c}{dt}=-\rho_1\int_{A_o}u_1 dA \quad \ldots (7)$$

where M_c is the air mass in the cavity, A_o is the orifice area and the subscript 1 denotes values at the cavity-orifice interface. Another cavity variable, the cavity volume V_c, can be obtained analytically from the diaphragm deformation (Equation 1)

$$V_c=\frac{\pi D_c^2}{4}\left[H-\frac{\Delta}{8}\mathrm{Sin}(2\pi ft)\right] \quad \ldots (8)$$

where D_c is the diameter of the cavity or diaphragm, and H is the height of the cavity.

To simplify the analysis, it is assumed that the fluid is stationary and the pressure is uniform inside the cavity. This assumption produces a negligible error when the cross-sectional area of the orifice is much smaller than that of the cavity cap. In addition, it is assumed that the compression and expansion process taking place in the cavity occurs instantaneously as the diaphragm oscillates. Both assumptions are valid when the dimensions of the actuator are much smaller than the wavelength of sound, a condition which is satisfied by the actuators studied in this work.

2.1.4 Solutions of the model

Equation (6) is nonlinear with respect to u_1 hence it can not be rearranged into a set of linear equation that are easy to solve. This problem is overcome by expressing the equation in the Δ form[11], which produces a tri-diagonal set of equations, enabling the use of the numerically efficient Thomas algorithm.

Equations (6) and (7) in fact are coupled and are solved using a predictor-corrector scheme that is second-order accurate in time. With the cavity mass and volume known, the density ρ_1 in the cavity can be readily calculated and the cavity pressure p_1 will then be obtained using the state equation for ideal gases (the air in the cavity is assumed to be isothermal). Finally, the velocity at the inlet and outlet of the orifice (u_1 and u_2) can be found from Equations (5) and (6).

In the simulation, a time step of two hundredth of a diaphragm oscillation cycle and 25 grid points across the orifice radius are used, which was found sufficient to capture the flow details to an acceptable degree of accuracy. The jet velocity to be used later in this paper is the space-averaged peak jet velocity during a diaphragm oscillation cycle which is calculated from u_2.

2.2 The dynamic incompressible model (DI model)

If the flow in the cavity is incompressible, the instantaneous volume flow rate displaced by the diaphragm is equal to that expelled through the orifice. Hence the space-averaged peak velocity at the orifice exit can be determined explicitly from Equation (1) without the need of modelling the flows inside the cavity and orifice duct as[7]

$$u_{peak_inv}=\frac{\pi}{4}\Delta f\left(\frac{D_c}{D_o}\right)^2 \quad \ldots (9)$$

This formula clearly shows that the peak jet velocity is proportional to the product of diaphragm oscillating frequency and amplitude for a given actuator. It also indicates that when the flow is incompressible the magnitude of the peak velocity is determined by the ratio between the cavity and the orifice diameter but not affected by the depth of the cavity and the orifice.

3.0 A PARAMETRIC STUDY OF SYNTHETIC JET ACTUATORS

With the aforementioned computational models, the effect of actuator geometry on the synthetic jet exit peak velocity can be investigated. To facilitate this study, a baseline actuator is chosen and its geometry is specified in Table 1. This actuator will be used in

https://doi.org/10.1017/S0001924000004681 Published online by Cambridge University Press

Table 1
Dimensions of the baseline synthetic jet actuator

Actuator parameters	Value
Orifice diameter (D_o)	0·5mm
Orifice depth (h)	0·5mm
Cavity diameter (D_c)	45mm
Cavity height (H)	10mm
Diaphragm peak-to-peak displacement (D)	0·01mm
Diaphragm oscillation frequency (f)	100Hz

a subsequent experimental study in which a detailed PIV measurement will be undertaken. The orifice depth of this actuator is chosen to be equal to the orifice diameter since it was found in a previous experiment that a ratio of orifice depth and diameter of 1 allows a strong and stable vortex ring to be formed[12].

3.1 Validation of the SC model

Before the detailed investigation began, the results obtained with the SC model and DI model were compared and calibrated against these produced by solving the full Navier-Stokes equations in FLUENT. Unsteady axisymmetric compressible numerical simulations were performed. For simplification, a velocity-inlet boundary condition was applied at the neutral position of the diaphragm instead of a moving boundary condition. Previous study showed that this simplification had a negligible effect on the jet velocity and the formation of vortex rings. The time-step used for the simulations was T/80. A sensitivity study undertaken previously confirmed that the choices of mesh size and time-step used in the present study were adequate[13]. According to experimental observations, the near field flow of all the selected cases was laminar. Therefore for the purpose of validating the magnitude of exit jet velocity predicted by the SC model, in the present study performing the FLUENT simulations using the laminar model is regarded as adequate. Further details about the simulations can be found in Tang and Zhong[13,14].

Since the dimensions of the actuator are much smaller than the wavelength of the sound (about 3·4m for the baseline case), the pressure variation inside the cavity is expected to be uniform and occur instantaneously. In addition, it was found in the experiments that the magnitude of pressure variations in the cavity may reach a few hundred Pascals when the Helmholtz resonance occurs. Therefore, despite the belief that acoustic events tend to be associated with pressure variations which could be too small to be resolved by a general purpose CFD packages like FLUENT, the Helmholtz resonance occurring in the synthetic jet actuator can still be simulated.

To facilitate the validation, orifice diameter D_o of the baseline actuator is allowed to vary from 0·1 to 2mm with an increment of 0·1mm while other parameters are kept the same. Figure 2 shows the variation of peak velocity with changing orifice diameter using the DI model, SC model and FLUENT respectively. It is seen that the results from the three models are in good agreement when the orifice diameter is greater than 1mm. However, the DI model predicts that the velocity will increase monotonically as the orifice diameter decreases towards zero. This trend is incorrect since the velocity is expected to fall as the orifice diameter decreases below a certain value such that the viscous effect in the orifice duct becomes significant. In contrast, the SC model (shown in open squares) shows that a maximum peak velocity exists around D_o = 0·5mm for this particular actuator. The location of this peak appears to be in a good agreement with the numerical results from FLUENT (shown in solid squares).

However, the SC model appears to over-predict the velocity magnitude in the region near the optimal orifice diameter. This over-prediction was also observed by Lockerby and Carpenter[9]. They

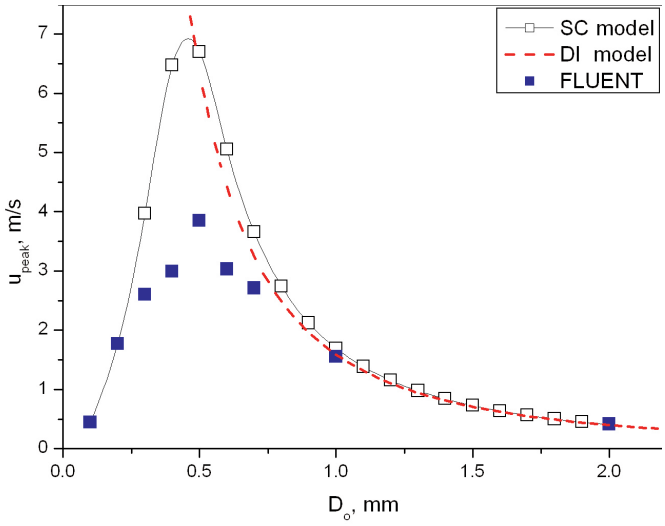


Figure 2. Peak velocity u_{peak} against orifice diameter D_o. All parameters are kept the same as those of the baseline actuator except D_o.

believed that this discrepancy arises from the inability of the SC model to model accurately the fluid dynamics near the inlet and outlet of the orifice duct. In reality, an accelerated region exists at both ends of the orifice, adding an extra length to the geometrical length of the orifice. Since this extra length is of the same order as the orifice diameter, typically about $0{\cdot}85D_o$[15], for an actuator with a relatively small orifice depth, it can significantly reduce the pressure gradient across the orifice, resulting in a lower exit velocity than that computed without considering it. Nevertheless, since it is still capable of predicting an optimal orifice diameter close to that given by FLUENT, the SC model is considered to be a useful tool for investigating the optimal geometry of synthetic jet actuators.

3.2 The effects of changing actuator geometry and operating parameters

The orifice diameter D_o is a key parameter of synthetic jet actuators and is usually used to define the non-dimensional parameters (such as Reynolds number and Strouhal number) for the jet flow. For a relatively high Reynolds number that is usually associated with a large D_o, the flow in the orifice is dominated by potential flow because the viscous layer is confined to the near-wall region. Provided the velocity through the orifice is low and the air in the cavity is incompressible, the DI model should be still accurate. As shown in Equation (9), in this case the peak jet velocity is inversely proportional to D_o^2.

However, as D_o decreases, the relative thickness of the viscous layer within the orifice duct increases and it eventually fills up the entire duct. If D_o decreases further, an increase in the input power to the actuator will not produce a proportional gain in jet velocity due to the significant viscous effect in the orifice duct. In this case, the flow can be regarded as quasi-steady and, according to the Hagen-Poiseuille formula[16], the highest instantaneous space-averaged exit velocity may be expressed as

$$u_{peak_v} \approx \frac{\Pi_{P_max} D_o^2}{32\mu} \qquad \ldots (10)$$

where Π_{P_max} is the maximum pressure gradient in the orifice and μ is the dynamic viscosity. Equation (10) indicates that the peak velocity is proportional to D_o^2.

https://doi.org/10.1017/S0001924000004681 Published online by Cambridge University Press

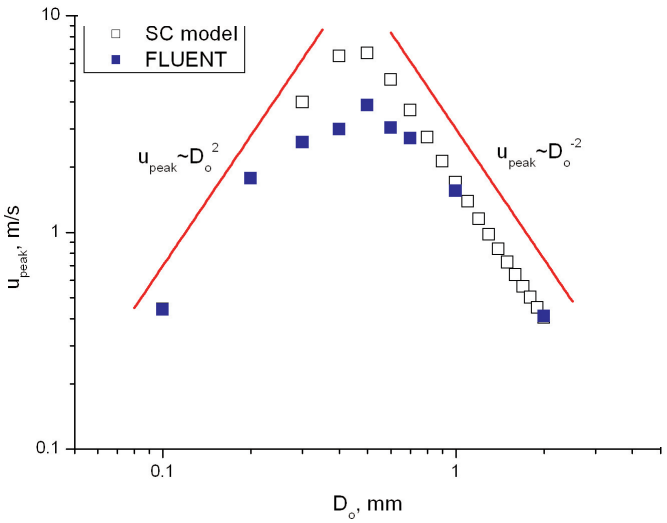


Figure 3. Peak velocity u_{peak} against orifice diameter D_o in logarithmic coordinates.

As shown in Fig. 2, the peak velocities predicted with the SC model are very close to those with the DI model when D_o is greater than 1mm. The data shown in Fig. 2 are re-plotted in the logarithmic coordinates in Fig. 3 in order to allow a closer examination of the relationship between peak jet velocity and the orifice diameters for the aforementioned two distinct flow regimes. It can be seen that the SC model is capable of capturing the expected features in the two flow regimes, i.e. that the peak velocity is proportional to D_o^2 for small orifice diameters and inversely proportional to D_o^2 for large orifice diameters.

Besides the orifice diameter D_o, the other parameters such as the cavity diameter D_c, cavity height H, orifice depth h, diaphragm oscillation amplitude Δ, and oscillation frequency f, also affect the exit peak velocity. To illustrate the influence of each individual parameter, both the SC model and DI model were used to compute the peak velocity by varying one parameter while keeping the other parameters constant. The results are shown in Fig. 4.

As shown in Fig. 4(a), the peak jet velocity initially appears to increase sharply as D_c increases since the volume displaced by the moving diaphragm increases proportionally to D_c^2. This increase becomes gradual as the D_c exceeds 50mm, and eventually the velocity starts to fall when D_c is greater than 90mm. For D_c less than 50mm, the prediction with the SC model follows that with the DI model closely, indicting that the flow in the cavity is essentially incompressible and the viscous effect in the orifice is not significant. From Fig. 4(a), an optimal D_c appears to exist which corresponds to the maximum peak jet velocity.

For incompressible flows, H and h are not expected to affect the magnitude of the exit velocity hence upeak versus H or h appears as a horizontal line in Fig. 4(b) and 4(c). However, they are seen to affect upeak significantly when the compressibility in the cavity is not negligible (see Fig. 4(b) and 4(c)). As H increases, the pressure variation produced by the diaphragm oscillation in the cavity decreases, resulting in a decrease in the exit velocity. Likewise, as h increases, the pressure gradient along the orifice duct decreases whereas the viscous effect in the orifice increases accordingly; a decrease in the exit velocity also results. However, optimal values of H and h appear to exist and the reason for this will become clearer later in this paper. It is worth noting that the trends of the peak velocity with varying H and the peak velocity with varying h are identical, if the value of h is multiplied by the ratio of H and h, which is equal to 20 in this case (see Fig. 4(b) and 4(c)). However, if the additional acceleration region in the orifice inlet and outlet were considered, it would be reasonable to expect that an effective orifice depth, which is equal to h plus the length of the acceleration regions, has the same effect as the cavity depth.

The oscillation frequency f is a measure of the extent of flow unsteadiness in the synthetic jets. At relatively lower frequencies, the peak velocity appears to increases linearly with f as predicted by the DI model (see Fig. 4(d)). Similar to D_o and D_c, an optimal frequency also exists for the actuator. The presence of an optimal frequency is a very important feature for a synthetic jet actuator and this will be discussed in the next section in more detail.

Within the range of diaphragm displacement (Δ) investigated here, the peak jet velocity increases as the diaphragm displacement increases. At small displacements, the peak velocity predicted by the SC model is linearly proportional to Δ which is consistent with the prediction with the DI model. For relatively large displacements, the rate of the velocity increase reduces due to the onset of compressibility and viscosity effects in the actuator (see Fig. 4(e)).

Based on the above discussions, optimal values of D_o, D_c, H, h and f appear to exist for a synthetic jet actuator. However, the optimal value of each parameter is expected to vary when any of the other parameters alters. As an example, the effects of changing D_c, H, h, Δ and f on how the maximum peak velocity varies with D_o is shown in Fig. 5 (the baseline case is plotted in open circles). It is seen that the optimal D_o increases with increasing D_c, H, h and f, but it does not change with Δ. The corresponding maximum peak velocity increases with increasing D_c, Δ and f, but decreases with H and h. Since the optimal D_o is invariant with Δ and varying H has the same effect on the peak velocity as varying h, to make the preceding discussion more concise, graphs illustrating the effects of changing Δ and h will not be shown.

4.0 RELATIONSHIP AMONG PARAMETERS AT THE OPTIMAL CONDITION

From the parametric study described in the previous section, it is found that the magnitude of the maximum peak jet velocity depends on four geometrical parameters (D_o, D_c, H and h) and two diaphragm operating parameters (f and Δ). In addition, except the diaphragm displacement (Δ), the optimal setting of one parameter changes when any of the other parameters alters. This implies that a relationship exists among all these parameters at the optimal design condition which yields the maximum peak velocity. Finding this relationship does not appear to be an easy task at the first sight. However, an investigation of the Helmholtz frequency of the actuator seems to provide a useful hint to this attempt.

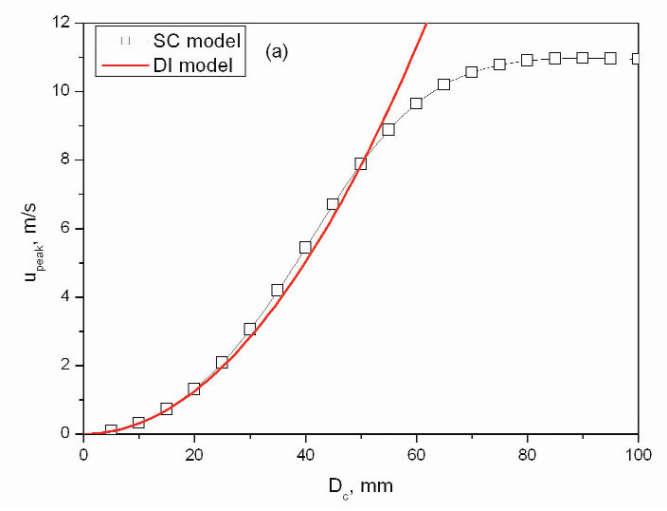
4.1 The Helmholtz frequency

Consider a container of air with an orifice. If disturbed, the column of air in the orifice tends to vibrate at a certain frequency because of the 'springiness' of the air inside the container. This resonance frequency is called the Helmholtz frequency and it depends on the geometry of the container and the orifice as well as the properties of air. Consisting of a cavity with an orifice and an oscillating diaphragm that provides a continuous source of excitation, a synthetic jet actuator potentially is a Helmholtz resonator. If the column of air in the orifice duct is treated as a dynamic system consisting of a mass suspended on a spring[17] and the compression and expansion process of the air in the cavity is assumed to be isothermal so as to be consistent with the assumption used in the SC model, the Helmholtz resonance frequency can be found as

$$f_H = \frac{a}{2\pi}\frac{D_o}{D_c\sqrt{\gamma H h}} \quad \ldots (11)$$

where a is the speed of sound and γ is the ratio of specific heat. At the Helmholtz frequency, a small pressure variation in the cavity is

https://doi.org/10.1017/S0001924000004681 Published online by Cambridge University Press



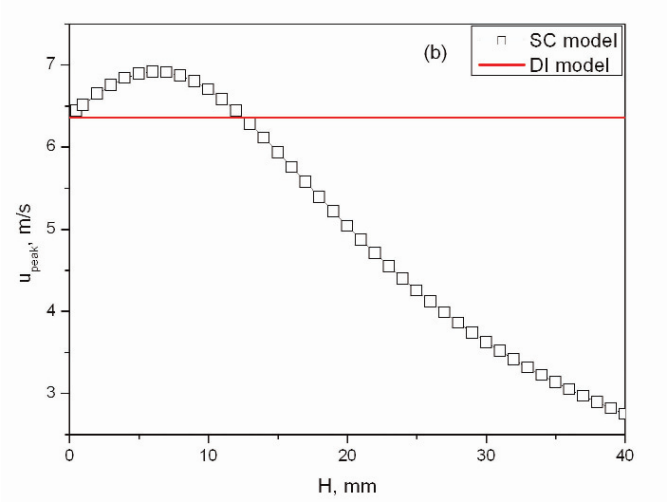
(a)

amplified to produce a large mass flow through the orifice. Hence, if the diaphragm natural frequency should be avoided in order to prolong the life span of a synthetic jet actuator, the actuator should operate at the Helmholtz frequency in order to obtain a reasonably high peak jet velocity.

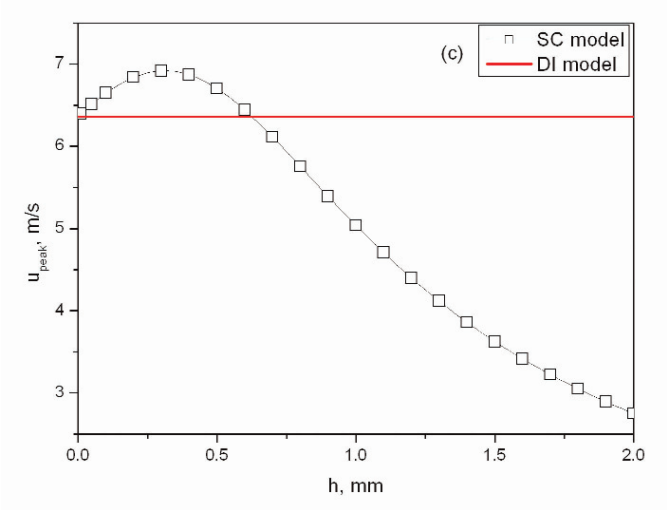
When the viscous effect in the orifice becomes significant, the resonance frequency calculated using Equation (11) becomes inaccurate. In this case, the friction exerted by the orifice wall on the column of air should be added to the dynamic equation as the damping term. If, for simplicity, the flow in the orifice duct is assumed to have the Hagen-Poiseuille velocity profile, the effect of viscosity on the Helmholtz frequency can be illustrated using the following formula

$$f = \frac{1}{2\pi}\sqrt{\frac{a^2 D_o^2}{\gamma H h D_c^2} - \frac{256\nu^2}{D_o^4}} \qquad \ldots (12)$$

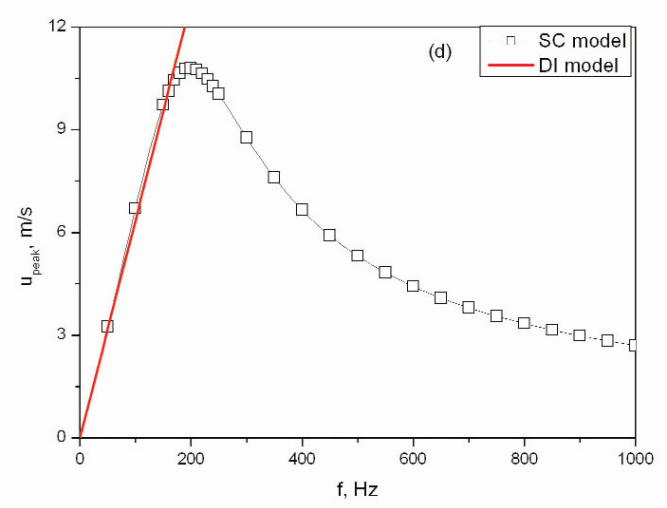
where ν is the kinematic viscosity. Compared to Equation (11), Equation (12) has an additional viscosity related term which acts to reduce the resonant frequency of the actuator. When the second term under the square root in Equation (12) becomes comparable to the first term, the Helmholtz resonance will be dampened by the viscous effect. Although not to be taken as a formula for calculating the



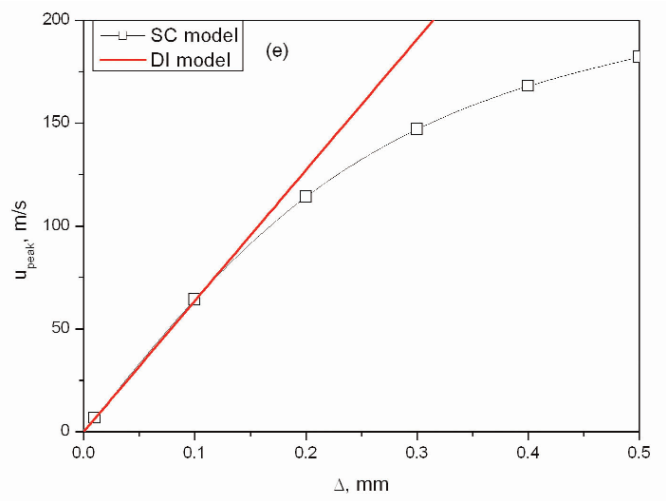
(b)



(c)



(d)



(e)

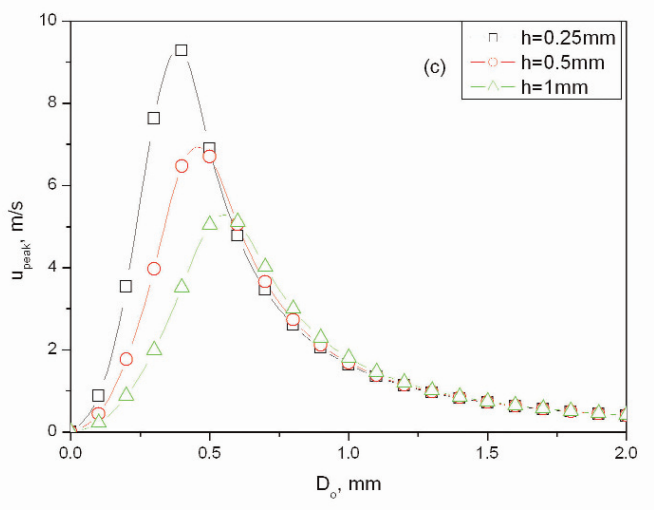
Figure 4. Peak velocity upeak against (a) D_c, (b) H, (c) h, (d) f, and (e) Δ.

https://doi.org/10.1017/S0001924000004681 Published online by Cambridge University Press

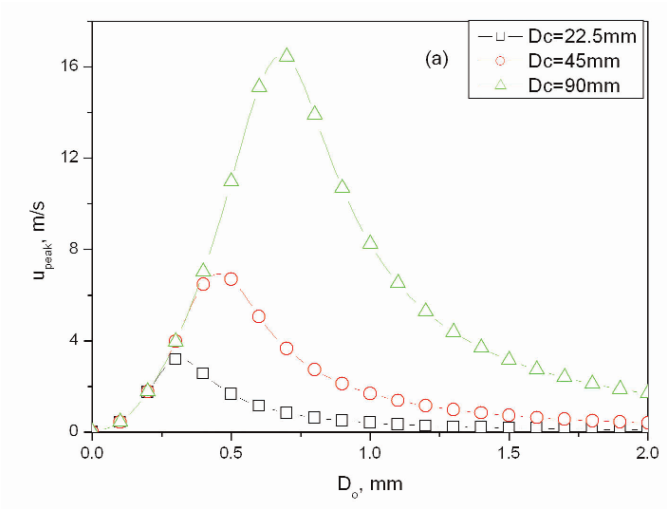
resonant frequency of the actuator, Equation (12) allows the effect of viscosity on the resonance frequency to be assessed. It is expected that the effect of viscosity becomes significant when the discrepancy in the frequencies predicted by Equation (11) and Equation (12) is appreciable.

4.2 The optimal condition for the non-Helmholtz resonance regime

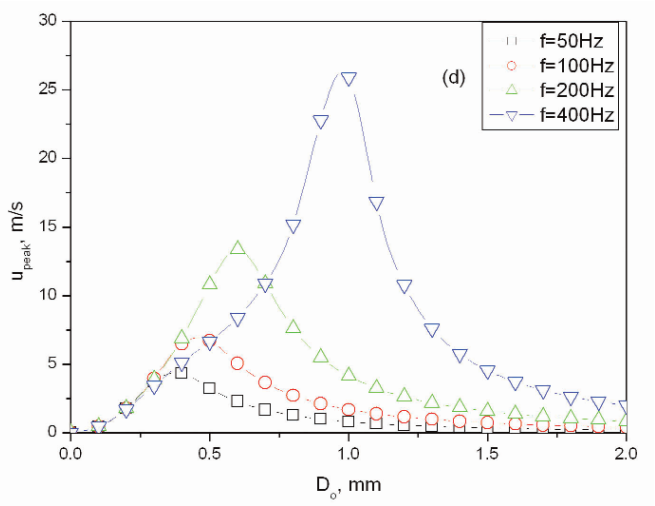
Equation (12) indicates that the friction in the orifice results in a reduction of the resonant frequency. When the second term is comparable to or greater than the first term, the resonance will be dampened. In this case, the synthetic jet actuator operates in a new regime, which is defined as the viscous flow regime. When the actuator is operating in this regime, the relationship among all the parameters at the optimal condition given in Equation (11) no longer applies. From Fig. 2, it can be seen that the optimal orifice diameter, which gives arise to the maximum peak velocity, is located around the region where the velocity curves predicted by the SC model and the DI model start to follow completely different trends. Hence it is reasonable to assume that at the optimal orifice diameter the velocities predicted by the SC model and the DI model are equal in



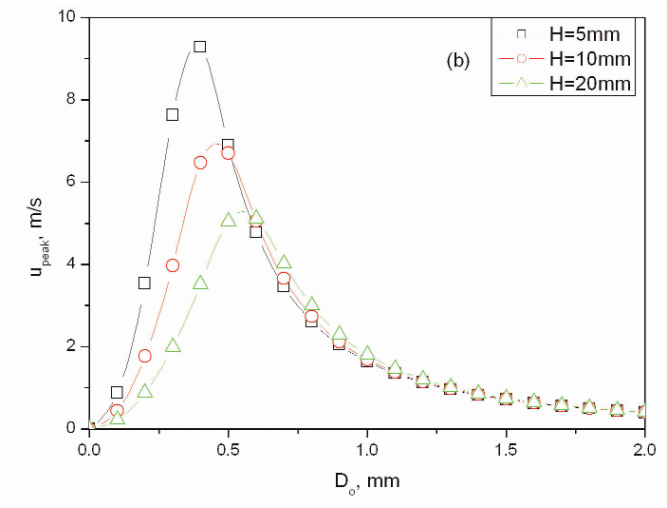
(c)



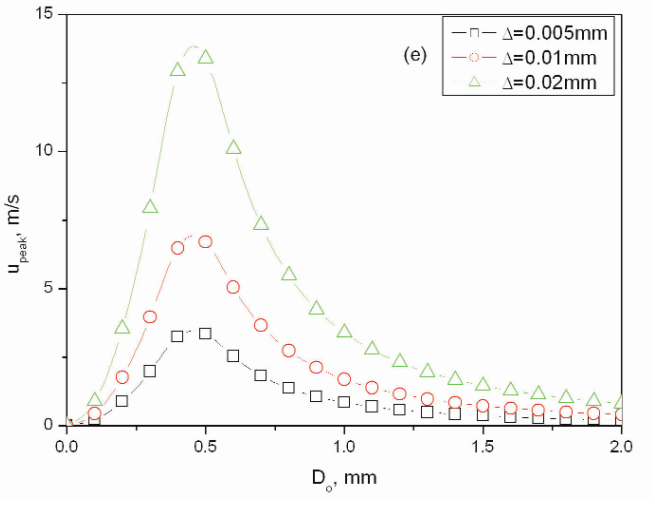
(a)



(d)



(b)



(e)

Figure 5. Peak velocity u_{peak} against D_o for cases varying (a) D_c, (b) H, (c) h, (d) f, and (e) Δ.

https://doi.org/10.1017/S0001924000004681 Published online by Cambridge University Press

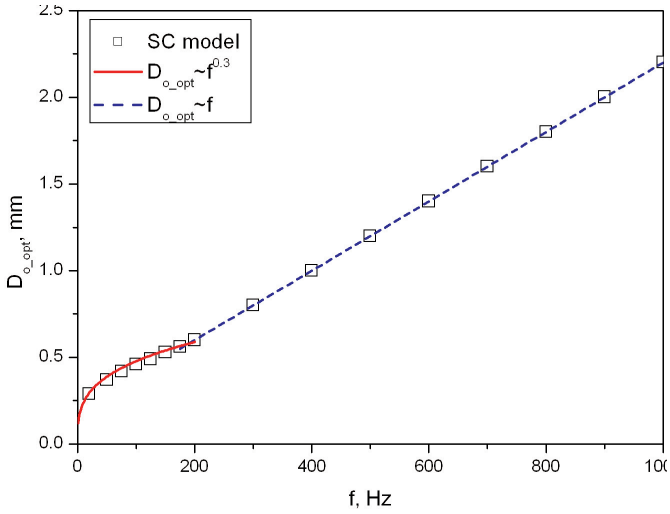


Figure 6. Optimal orifice diameter D_o against oscillation frequency f.

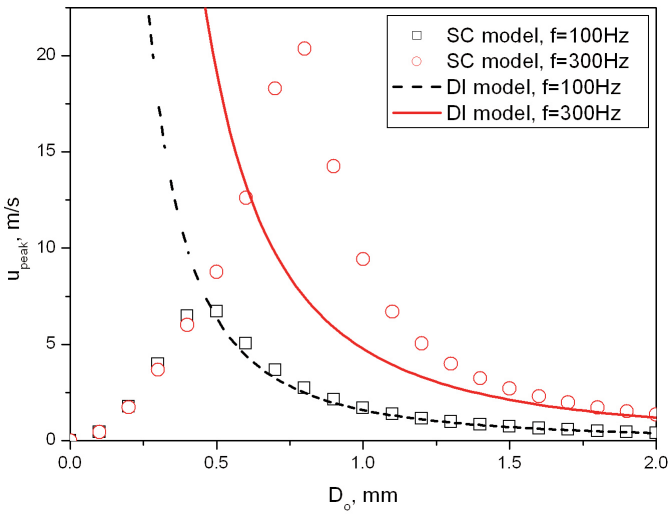


Figure 7. Comparison between the velocities predicted by the SC model and the DI model for f = 100Hz and 300Hz.

magnitude (this criterion was used by Carpenter and Lockerby[9] to select the optimal orifice diameter for their actuator). Based on this criterion, the relationship among the parameters at the optimal condition in the viscous flow regime can be obtained. This condition should correspond to the critical point at which the boundary layers developing along the opposite walls of the orifice duct begin to merge.

Assume that the cavity pressure is P_a (ambient pressure) when the diaphragm is at its neutral position, and that the cavity pressure is at its highest value when the cavity is at its minimum volume. When the viscous effect is significant in the orifice duct, the maximum pressure gradient Π_{P_max} along the duct can be estimated as

$$\Pi_{P_max} \approx \frac{P_{max} - P_a}{h} = \beta \frac{P_a \Delta}{8Hh} \quad \ldots (13)$$

where β is a correction factor and it is not a constant but dependent on the ratio of cavity diameter D_c to orifice diameter D_o, diaphragm displacement Δ, and oscillation frequency f. For an actuator which operates in the viscous flow regime or at the frequency far from the Helmholtz frequency, β is less than 1. Assuming the flow process in the cavity is isothermal and substituting Equation (13) into Equation (10), we get

$$u_{peak_v} \approx \beta \frac{P_a D_o^2 \Delta}{256 \mu Hh} = \beta \frac{a^2 D_o^2 \Delta}{256 \gamma \nu Hh} \quad \ldots (14)$$

Matching the space-averaged peak velocity in the inviscid and the viscous regimes by equating Equation (9) to Equation (14), we get

$$\frac{\pi}{4} \Delta f \left(\frac{D_c}{D_o} \right)^2 = \beta \frac{a^2 D_o^2 \Delta}{256 \gamma \nu Hh} \quad \ldots (15)$$

Equation (15) can be rearranged to provide an approximate relationship between the optimal frequency and the actuator geometrical parameters in a similar form as Equation (11) for the viscous flow regime,

$$f_{nonH} = \beta \cdot \frac{a^2}{64 \pi \gamma \nu} \cdot \frac{D_o^4}{Hh D_c^2} \quad \ldots (16)$$

4.3 Validation of the optimal conditions

Equations (11) and (16) are the relations that the parameters of an actuator are expected to satisfy in order to achieve the maximum peak velocity in the Helmholtz resonance regime and the viscous flow regime, respectively. To check the validity of these two relations, the numerical results are analysed. Figure 6 shows the optimal D_o versus frequency while keeping the other geometrical parameters constant. Data fitting reveals that the optimal D_o varies linearly with f when f > 200Hz. The observed linear relationship between f and D_o conforms to Equation (11) for the Helmholtz resonance regime. The relationship between the optimal D_o and f is clearly non-linear for f < 200Hz. Curve fitting of the non-linear relation for f < 200Hz reveals that the optimal D_o is proportional to $f^{0.3}$, which is close to the prediction of Equation (16) for the viscous flow regime, where D_o is proportional to $f^{0.25}$.

The variations of the peak velocity upeak are plotted against D_o for f = 100 and 300Hz in Fig. 7. It is seen that at f = 100Hz, the velocity predicted with the DI model matches closely to the velocity predicted with the SC model when D_o is relatively large (> 0·5mm). In addition, the point corresponding to the maximum peak velocity lies very close to the point where the prediction by the DI model departs from that by the SC model. This observation is consistent with the assumption that is used to derive the optimal condition for the viscous flow regime. In contrast, the point corresponding to the maximum peak velocity lies above the DI model prediction for f = 300Hz. The reason for this is that at this condition Helmholtz resonance occurs and the DI model, which estimates the exit velocity based on incompressible principle, does not include the additional gain in jet velocity due to Helmholtz resonance in the cavity. It is worth mentioning that the optimal orifice diameter corresponding to the maximum peak jet velocity obtained from Fig. 7 is 0·46mm and 0·77mm at f = 100Hz and 300Hz, respectively. They are very close to the values (0·44mm and 0·69mm) estimated using Equations (11) and (16).

Lockerby and Carpenter[9] believed that the optimal D_o should be located at the intersection point between the velocity curve predicted by the SC model and that by the DI model, even when Helmholtz resonance occurs. They thought that the solution from the SC model becomes invalid if the peak velocity predicted is greater than that given by the DI model, since the least energy output will be preferred by the system. However, the results from this study suggest that, due to the presence of Helmholtz resonance, the exit velocity can be much greater than the value predicted by the DI model. This claim is also supported by unpublished experimental evidence. A hot-wire experiment was performed on an actuator with D_o = 2mm, D_c = 30mm, H = 4mm, h = 1.5mm at Δ = 0·02mm. According to Equation (11) the Helmholtz frequency is about 1,240Hz for this actuator. The experiment showed that the resonance frequency was 1,000Hz and the peak velocity measured was 11ms^{-1},

https://doi.org/10.1017/S0001924000004681 Published online by Cambridge University Press

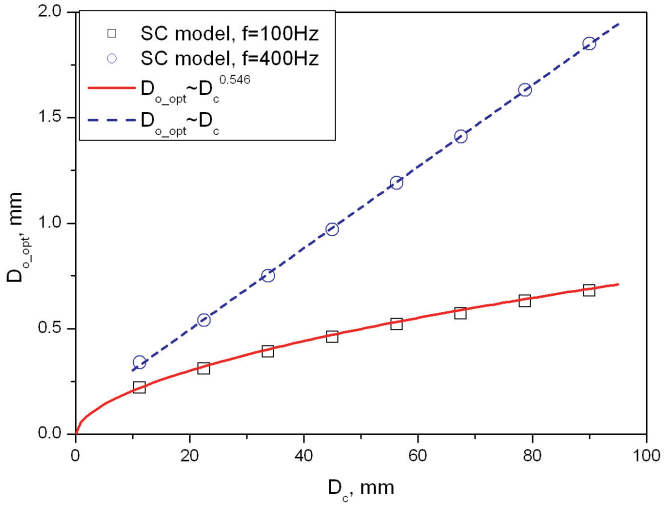


Figure 8. Optimal orifice diameter D_o against cavity diameter D_c.

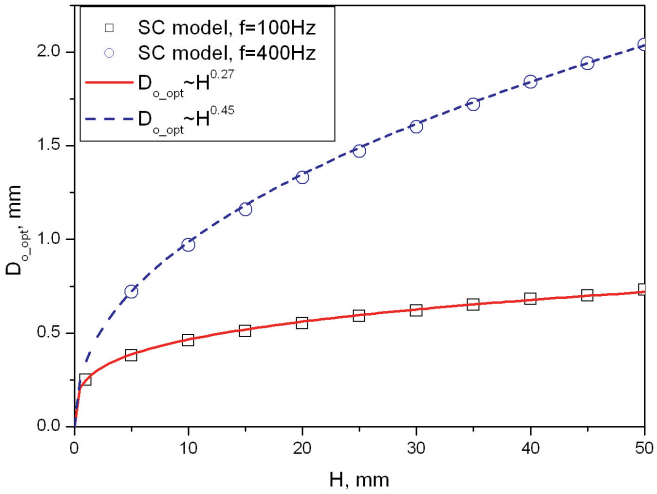


Figure 9. Optimal orifice diameter D_o against cavity height H.

which is significantly greater than the velocity of 3·5ms^{-1} predicted by the DI model (Equation 9).

All these evidences seem to be in line with the presence of the two actuator operating regimes. Further evidence can be acquired by examining the variations of the optimal D_o against D_c. As shown in Fig. 8 and 9, at f = 400Hz where the optimal velocity is in the Helmholtz resonance regime, the optimal D_o predicted by the SC model is linear to D_c and approximately proportional to $H^{0.45}$, close to $H^{0.5}$ in Equation (11). But at f = 100Hz where the optimal velocity is in the viscous flow regime, the optimal D_o is approximately proportional to $D_c^{0.546}$ and $H^{0.27}$, close to D_c 0·5 and $H^{0.25}$ in Equation (16). The discrepancy for the f = 100Hz case is largely due to the fact that the correction factor β was taken as unity for simplicity in calculation.

5.0 DESIGN CONSIDERATION FOR SYNTHETIC JET ACTUATORS

5.1 The relation between the maximum peak jet velocity and actuator parameters

Although Equations (11) and (16) specify the relationship between the geometrical and operating parameters that would yield a maximum peak jet velocity, the choice of these parameters is not unique hence the resultant magnitude of the maximum peak jet velocity can vary. In this section, an attempt is made to establish the relations between the maximum peak velocity and the actuator geometrical and operating parameters in order to assist the selection of these parameters. To simplify the analyses, the diaphragm displacement Δ is assumed to be very small such that the peak velocity is linearly proportional to Δ (see Fig. 4(e)). Also based on the results shown in Fig. 4(b) and 4(c), the orifice depth h has the same effect on the velocity as the cavity height H. Therefore, only the effects of orifice diameter D_o, cavity diameter D_c, cavity height H and oscillation frequency f on the maximum peak velocity are studied in this section.

For the Helmholtz resonance regime, all the combination of parameters should comply with the Helmholtz condition (Equation 11). This indicates that if one parameter is altered some of the other parameters have to change accordingly in order to satisfy this condition. If only two parameters are allowed to be changed each time, the resultant maximum peak velocity will vary with these two parameters. However, these two parameters are also linked to each other via the Helmholtz condition. To simplify the analyses, D_o is fixed as one of the two parameters and the other parameter is one of the remaining parameters, i.e. D_c, H or f. By investigating all the possible combination of the parameter pairs, the relation between each individual parameter (D_o, D_c, H or f) and the maximum peak velocity can be studied separately.

Figure 10(a) shows the maximum peak velocity against D_o for three different cases: varying f, D_c and H respectively. It can be seen that, in both the f varying and D_c varying cases, the maximum peak velocity is linear to the optimal D_o. And for H varying case, the optimal velocity is proportional to the optimal $D_o^{-0.9}$ which can be approximated as D_o^{-1}. With the known relationship between D_c, H or f and D_o inferred by the Helmholtz condition, the optimal velocity is therefore found to be approximately proportional to f, D_c and $H^{-0.5}$ respectively. Simply arranging these results, a relation between the maximum peak velocity and the other parameters can be obtained

$$u_{peak_opt} \propto \frac{\Delta f D_c}{\sqrt{Hh}} \quad \ldots (17)$$

It has an alternative form if combined with Equation (11), making both f and D_c implicit

$$u_{peak_opt} \propto \frac{a\Delta D_o}{Hh} \quad \ldots (18)$$

Likewise, for the viscous flow regime, the relations between the optimal velocity and the actuator parameters can be obtained in a similar way. The maximum peak velocity against D_o for the same three cases is plotted in Fig. 10(b). Curve fitting reveals that the maximum peak velocity is approximately proportional to D_o^2 in f varying and D_c varying cases, whereas it is approximately proportional to D_o^{-1} in H varying case. With the known relationship between D_c, H or f and D_o inferred in Equation (16), the maximum peak velocity is therefore approximately proportional to $f^{0.5}$, D_c, and $H^{-0.25}$, respectively. A relation between the optimal velocity and the parameters can also be obtained

$$u_{peak_opt} \propto \Delta f \left(\frac{D_c}{D_o}\right)^2 (Hh)^{1/4} \quad \ldots (19)$$

Note, the above relation is obtained by best fitting the data and the dimension of the right-hand side term has not been made identical to that of velocity. Equation (19) has an alternative form if combined

https://doi.org/10.1017/S0001924000004681 Published online by Cambridge University Press

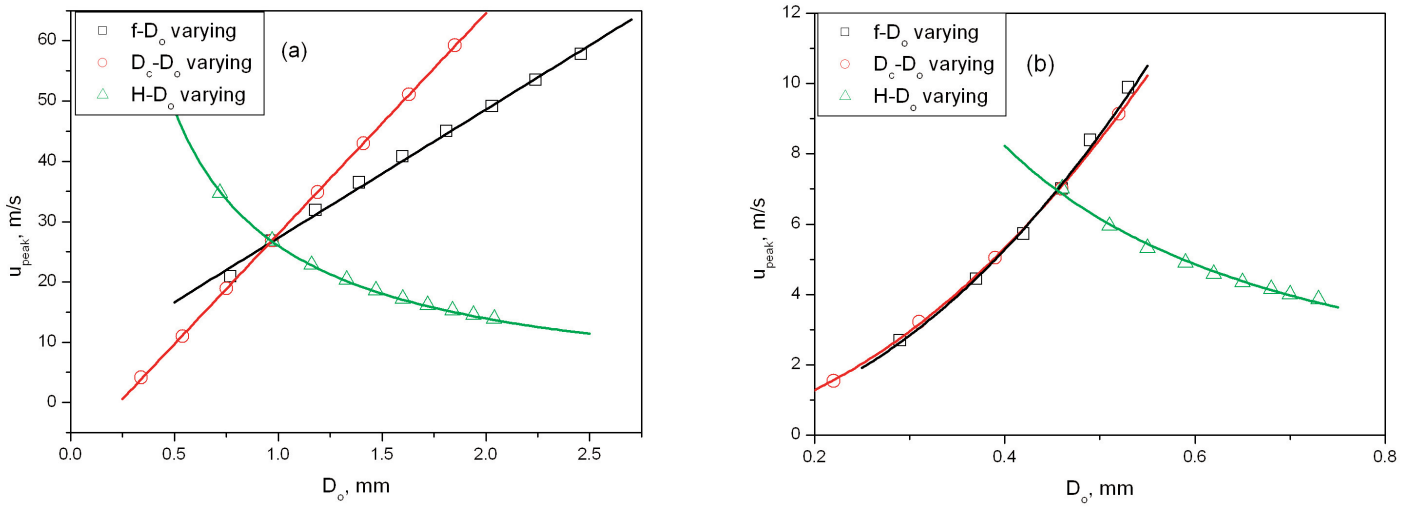


Figure 10. Optimal velocity against orifice diameter D_o for (a) the Helmholtz resonance regime and (b) the viscous flow regime.

with Equation (16), making both f and D_c implicit

$$u_{peak_opt} \propto \frac{a^2}{\nu} \cdot \frac{\Delta D_o^2}{(Hh)^{3/4}} \quad \ldots (20)$$

5.2 Additional factors to be considered

It should be mentioned that the SC model and Equations (11) and (16) were developed based on the isothermal assumption, which is adequate for actuators operating at relatively low frequencies, say less than 1,000Hz. At higher frequencies, the compression and expansion process in the cavity is more adequately regarded as adiabatic and hence it is accompanied by a considerable amount of temperature variations. Furthermore, the accelerated region existing at the two ends of the orifice, which adds an extra length to geometrical length of the orifice, was not considered. According to the existing literature[15], the effect of this extra length can be conveniently taken into account by introducing an effective orifice length, i.e. $h' = h + \alpha D_o$, where $\alpha = 0{\cdot}85$.

If the above two factors are taken into account, Equations (11) and (16) can be rewritten as

$$f_H = \frac{a}{2\pi} \frac{D_o}{D_c \sqrt{Hh'}} \quad \ldots (21)$$

$$f_{nonH} = \beta \cdot \frac{a^2}{64\pi\nu} \cdot \frac{D_o^4}{Hh' D_c^2} \quad \ldots (22)$$

The relations between the optimal peak velocity and the actuator parameters for the Helmholtz resonance regime and viscous flow regime (Equations 18 and 20) can be expressed accordingly as

$$u_{peak_opt} \propto \frac{a\Delta D_o}{Hh'} \quad \ldots (23)$$

$$u_{peak_opt} \propto \frac{a^2}{\nu} \cdot \frac{\Delta D_o^2}{(Hh')^{3/4}} \quad \ldots (24)$$

Applying Equation (21) to the actuator which was tested in an experiment as mentioned in Section 4.3, one gets a Helmholtz resonance frequency of 1,008Hz. This value is closer to the experimental value of 1,000Hz than that predicted with Equation (11) largely due to the use of the effective orifice length.

5.3 Design considerations for synthetic jet actuators

Given the relationships between the maximum peak velocity and the actuator geometrical and operating parameters (Equation 23 and Equation 24), it is now possible to make some recommendations for optimizing the design of synthetic jet actuators used for flow separation control on aircraft. An application of interest is to delay flow separation on the flap of a multi-element high-lift system at take-off and landing by employing an array of synthetic jets.

For a known boundary layer on an aircraft wing, the orifice diameter is often set as not being greater than 5%~20% of the local boundary layer thickness so as to minimize the disturbances to the flow. Constraints on the maximum orifice size may also be imposed to ensure structural integrity. According to the aforementioned analyses, the maximum peak jet velocity is proportional to D_o in the Helmholtz resonance regime (Equation 23) or D_o^2 in the viscous flow regime (Equation 24). It implies that the orifice diameter D_o should be made as large as possible within the above physical constraints.

Given the local free stream velocity and the boundary layer thickness, the frequency range that the actuators are expected to operate is also determined (often in the kilohertz range) so as to ensure adequate spacing between the consecutive structures produced by the synthetic jets (typically of the order of a local boundary layer thickness). Ideally the actuator should be operated at either the Helmholtz frequency or the frequency specified in Equation (16) to obtain the highest peak jet velocity possible for a given input to the actuator. It would be possible to tune this frequency closer to the desirable frequency range set by the aircraft take-off or landing condition by altering the cavity diameter D_c, cavity height H and orifice depth h. Smaller H and h are often advantageous since both the maximum peak jet velocity and the optimal frequency of the actuator are higher. The main constrain on H and h comes from the requirement for ensuring the structural integrity and reducing manufacturing costs. Although a smaller D_c will result in a higher optimal actuator frequency and a lighter actuator, the magnitude of jet velocity will reduce. Hence the choice of D_c requires a balanced consideration between these two opposing factors.

For the purpose of flow separation control on an aircraft, the peak jet velocity should be comparable to the local free stream velocity over the wing. This requirement sets the peak jet velocity that the actuator is expected to produce. Although the SC model can not be used to predict the actual magnitude of the maximum peak jet velocity, it allows the optimal operating frequency and the geometrical parameters of actuators to be determined for a given diaphragm

https://doi.org/10.1017/S0001924000004681 Published online by Cambridge University Press

displacement. The diaphragm displacement can be then varied to adjust the jet velocity relative to the local free stream velocity. CFD codes which solve the full Navier-Stokes equations should be used to predict the achievable peak jet velocity more accurately.

6.0 CONCLUSIONS

In this paper, a simple static compressible model for circular synthetic jet actuators is described. It was used to investigate the effect of changing actuator geometrical and operating parameters on the magnitude of peak jet velocity at the orifice exit of an actuator whose diaphragm displacement and frequency are allowed to vary independently. An attempt was made to establish the relation among these parameters at the optimal design condition which yields the maximum peak jet velocity at a given diaphragm displacement. A procedure for designing synthetic jet actuators for flow separation control on an aircraft wing is also proposed. The key conclusions from this study are summarised as follows:

1. The magnitude of the maximum peak jet velocity depends on four geometrical parameters (D_o, D_c, H and h) and two diaphragm operating parameters (f and Δ). Except the diaphragm displacement (Δ), an intricate relation exists among all these parameters at the optimal actuator design condition.
2. Depending on the flow conditions inside the orifice duct, the actuator may operate in two distinct regimes, i.e. the Helmholtz resonance regime and the viscous flow regime. In the Helmholtz resonance regime, the resultant synthetic jet is generated by the mass physically displaced by the oscillating diaphragm coupled with the Helmholtz resonance in the actuator. In the viscous flow regime, the Helmholtz resonance is completely damped by viscous effect such that the jet is produced by the diaphragm oscillation alone.
3. In the Helmholtz resonance regime, the combination of the actuator parameters satisfies the Helmholtz condition (Equation 11) at the optimal design condition. This maximum peak jet velocity can be higher than the value predicted by the DI model due to the presence of Helmholtz resonance in the cavity. In the viscous flow regime, the combination of the actuator parameters satisfies the relation stated in Equation (16) at the optimal design condition.
4. By best-fitting the computational data, the qualitative relations between the maximum peak jet velocity and the actuator geometrical and operating parameters for the two regimes (Equations (18) and (20) are obtained. These relations combined with the relation that the actuator parameters should satisfy at the optimal design condition in the corresponding actuator operating regime, can be used to design synthetic jet actuators for a given flight condition.

ACKNOWLEDGMENTS

The authors would like to thank Dr Duncan Lockerby for the valuable discussions regarding the static compressible model. They would also like to thank Mr. Fushui Guo for providing the experimental data used in Section 4.0.

REFERENCES

1. AMITAY, M., SMITH, B.L. and GLEZER, A. Aerodynamic flow control using synthetic jet technology, 1998, AIAA Paper 98-0208.
2. CROOK, A., SADRI, A.M. and WOOD, N.J. The development and implementation of synthetic jets for the control of separated flow, 1999, AIAA paper 99-3176.
3. MCCORMICK, D.C. Boundary layer separation control with directed synthetic jets, 2000, AIAA paper 2000-0519.
4. GLEZER, A. and AMITAY, M. Synthetic jets, *Annu Rev Fluid Mech*, 2002, **34**, pp 503-29.
5. KRAL, L.D. Active flow control technology, 1998, ASME Fluids Engineering Division Technical Brief.
6. HO, C.M. and TAI, Y.C. Micro-electro-mechanical-systems (MEMS) and fluid flows, *Annu Rev Fluid Mech*, 1998, **30**, pp 579-612.
7. TANG, H. and ZHONG, S. Incompressible flow model of synthetic jet actuators, *AIAA J*, 2006, **44**, (4), pp 908-912.
8. RATHNASINGHAM, R. and BREUER, K.S. Coupled fluid-structural characteristics of actuators for flow control, *AIAA J*, 1997, **35**, (5), pp 832-37.
9. LOCKERBY, D.A. and CARPENTER, P.W. Modeling and design of microjet actuators, *AIAA J*, 2004, **42**, (2), pp 220-27.
10. TIMOSHENKO, S. and WOINOWSKY-KRIEGER, S. *Theory of Plates and Shells*, 1959, Second Edition, McGraw-Hill Book Company, London.
11. FERZIGER, J.H. *Numerical Methods for Engineering Applications*, 1998, Second Edition, Wiley-Interscience, New York.
12. CROOK, A. and WOOD, N.J. A parametric investigation of a synthetic Jet in quiescent conditions, 2000, Ninth International Symposium on Flow Visualization, Edinburgh, UK.
13. TANG, H. and ZHONG, S. 2D numerical study of circular synthetic jets in quiescent flows, *Aeronaut J*, February 2005, **109**, (1092), pp 89-97.
14. TANG, H. and ZHONG, S. Characteristics of small-scale synthetic jets — numerical investigation, IUTAM Symposium on Flow Control and MEMS, 2006, London, UK.
15. KINSLER, L.E., FREY, A.R., COPPENS, A.B. and SANDERS J.V. *Fundamentals of Acoustics*, 1982, Third Edition, John Wiley & Sons, New York.
16. WHITE, F.M. *Viscous Fluid Flow*, 1991, Second Edition, McGraw-Hill Book Company, New York.
17. DOWLING, A.P. and FFOWCS WILLIAMS, J.E. *Sound and Sources of Sound*, 1983, Ellis Horwood, Chichester, UK.

https://doi.org/10.1017/S0001924000004681 Published online by Cambridge University Press